Emulating a Software Defined LTE Radio Access Network Towards 5G

Inês da Silva Santos
ines.s.santos@tecnico.ulisboa.pt

Instituto Superior Técnico, Lisboa, Portugal

June 2018

Abstract

This work evaluates the performance of a Software Defined Network (SDN) and the respective OpenFlow (OF) protocol, when supporting a Long Term Evolution (LTE) Radio Access Network (RAN). The main objective is to understand the impact of the new network technologies and the new network architecture, using a SDN based LTE network (when compared to conventional LTE networks), in a solution towards Fifth Generation (5G) implementation. Several simulations were performed using the SDN emulator Mininet-Wifi platform, which was adapted to produce use cases regarding a SDN based LTE topology. This platform uses WiFi as radio technology. However, and since this is an open source platform, changes were introduced in order to include a LTE RAN parametrization based on LTE technology standards. The latency and throughput are the used Quality of Service (QoS) performance metrics.

The throughput results led to a 54 % and 158 % spectral efficiency increase regarding the ITU requirement for urban and rural environments respectively, for a LTE Radio Access system reference from 3GPP. Latency results were also obtained for the same reference scenario achieving, in the urban environment, average values of 21-22 ms, close to the 3GPP requirement for LTE of 20 ms; on the other hand, for the rural environment the average latency values were around 122 ms. The latency was also analyzed according to the SNR and the packet size. The latency was then measured according to the *drive-tests* scenario in order to compare the emulator results with real network measurements. The emulator presented better latency results than the *drive-tests* despite the different latency curve behaviour. At last, the latency was measured only in the backhaul/core network where the SDN influence is notorious, and the emulator reached 40.18 % lower latency.

Keywords: SDN, C-RAN, OpenFlow, 5G, throughput, latency, RTT

1. Introduction

The 5th Generation of Mobile Communications (5G) currently being discussed and expected to be standardized and deployed until 2020 [13], aims to provide a wide range of new applications, not only because of the improvements in latency, throughput or capacity, but also due to an entire different way of thinking the network, in both architecture and implementation fields. In order to face these challenges, new solutions based on intelligence, automation and flexibility in control and interfaces management are essential. In this new mobile generation, the network architecture will suffer some adjustments concerning the radio access component, with a centralized RAN, composed by base stations antennas (Remote Radio Heads, RRHs) located near the users and processing units (Baseband Units, BBUs) concentrated in a data centre.

Along with the 5G, a new trend emerged and is expected to be a promising approach for mobile networks - Software Defined Networks (SDNs). SDN intends to minimize hardware constraints and to abstract lower level functions, by moving them to a standardized control plane, responsible for the management of the network behavior, through Application Program Interfaces (APIs). From a software-based centralized control plane, network administrators can provide services to the network despite the connected hardware components. SDN can be used to provide an overall framework which enables 5G to work across a control plane.

In this paper, a simplified SDN enabled 4G cellular network is considered, as a step towards the 5G concept, to meet high users expectations and respect the network requirements. Its performance was evaluated in terms of latency and throughput via network simulation in Mininet-Wifi [15], a Software-Defined Wireless Network emulator that enables the testing of a LTE RAN over SDN technology.

The paper is organized as follows. Section II describes the 5G vision and network architecture, and the emerging concepts of SDN and OpenFlow. The LTE Radio Frequency (RF) system scenario, which served as reference to setup the RAN, is described in

Section III; this section also presents the network configuration implemented in Mininet-Wifi, along with this platform description and the performed network tests. In Section IV, the results are presented and compared with typical LTE values. Finally, in Section V, conclusions are drawn.

2. Background

The Centralized Radio Access Network (C-RAN) is a centralized, cloud-based new cellular network architecture that can be adopted by Mobile Network Operators (MNOs) to improve the quality of service with reduced capital expenditure Capital expenditure (CAPEX), operating expenditure Operational expenditure (OPEX), and energy consumption [19].

Figure 1 shows an example of a C-RAN mobile LTE network. The fronthaul part spans from the RRHs sites to the BBU Pool. The backhaul connects the BBU Pool with the mobile core network. At a remote site, RRHs are co-located with the antennas. RRHs are connected to the high performance processors in the BBU Pool through low latency, high bandwidth optical transport links [4]. Digital baseband are sent between a RRH and a BBU.

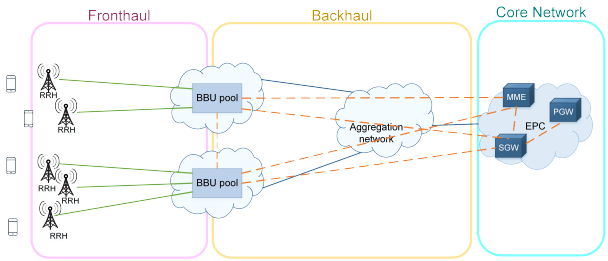

Figure 1: C-RAN LTE mobile network (adapted from [4])

According to the Open Networking Foundation (ONF) [8], SDN is considered one of the most promising technologies to attain virtual networks, where the network control plane is decoupled from the data plane and is directly programmable. Network intelligence is logically centralized in the software-based SDN controller, built by multiple physical and virtual components, but still behaves like a single node.

The SDN architecture is divided in three layers and is represented in Figure 2. In [10], the Application layer represents the functional applications of the network as services provided by the network operator, like access control, traffic/security monitoring and energy-efficiency or, in other words, end-user business applications that consume SDN communications services. The Control layer consists in logically centralized controllers, that supervise the network and operate on the forwarding devices through an open interface. The Infrastructure layer involves the physical network elements and devices that provide packet switching and forwarding, such as virtual switches and physical switches.

The network applications communicate their requirements towards the controllers via software interfaces, the Northbound APIs. The Southbound API is especially important since it is the one responsible for the communication between the control and data planes. The best known, and whose analysis will be addressed below, is OpenFlow. These software interfaces are open source-based.

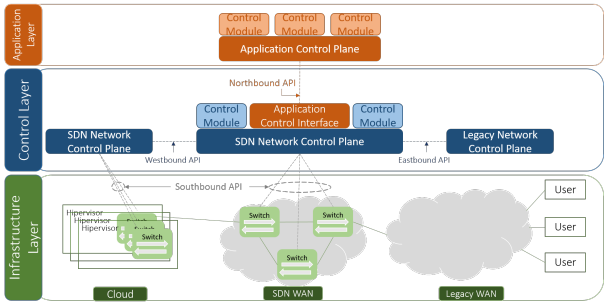

Figure 2: SDN overview (adapted from [10]).

The OpenFlow specification is controlled and defined by ONF [9], which is led by a board of directors from seven companies that own and operate some of the largest networks in the world (Deutsche Telekom, Facebook, Google, Microsoft). In [9], the OpenFlow is defined as the protocol that provides software-based access to the flow tables, that instruct switches and routers on how to direct network traffic. Using these flow tables, administrators can quickly change the network layout and traffic flow. An OpenFlow switch consists on one or more flow tables and a group table, which performs packet lookups and forwarding, and an OpenFlow channel to communicate with an external controller. This controller manages the switch via OpenFlow protocol, being able to add, update and delete flow entries in the flow tables. The structure of the flow tables is presented in Figure 3 and their details can be found in [7].

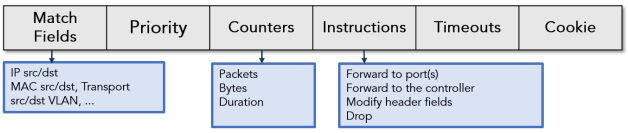

Figure 3: OpenFlow flow entry.

3. LTE over SDN Implementation

This chapter presents the implemented SDN scenario as well as all the 3GPP LTE references used in order to simulate a LTE over SDN network in Mininet-WiFi, which is originally specified for WiFi. Furthermore, the LTE features implementation in the emulator and the SDN used mechanisms are detailed.

3.1. Emulator Description

Mininet-Wifi [15] emerged as a dependency of Mininet [18], an OpenFlow/SDN emulator capable of add virtualized stations and access points, based on the stan-

dard Linux wireless drivers and the 80211_hwsim [1] wireless simulation driver. This emulator uses the SDN paradigm, which allows network administrators to specify the behaviour of the network in a logic centralized manner through the use of a controller that operate over the forwarding devices through the OpenFlow protocol.

The mobile network topology implemented in the emulator has two parts: the wireless network (representing a LTE RAN network combined with C-RAN concepts) and the wired network (constituted by SDN OpenFlow enabled switches responsible for the data plane functions). The control plane is the responsibility of the controller. The wireless network is composed by the base station antennas, here represented by **RRHs**, and the mobile users, the **UEs**.

The emulator runs in the Linux Operating System (OS), and the system memory in Linux can be divided into two distinct regions:

- The **kernel space** where the kernel (core of the operating system) executes and provides its services. In the kernel-space the module mac80211_hwsim is responsible for creating virtual wireless interfaces, in this case the RRHs and UEs. Moreover, in the kernel-space, MLME (Media Access Control Sublayer Management Entity) is realized in the UEs side.

- The **user space** is a set of memory locations in which user processes run. A process is an executing instance of a program. In the user-space the *hostapd*[1] is responsible for the MLME functions in the RRH side. Also, another important utility is TC (Traffic control), which is used to configure the Linux kernel packet scheduler, responsible for controlling the data rate, delay, latency and loss, applying these attributes in virtual wireless interfaces of UEs and RRHs, representing with higher fidelity the behaviour of the real world networks.

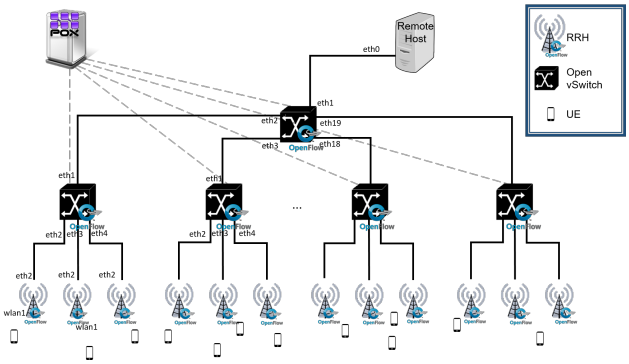

Figure 4: Mininet-Wifi network implementation

[1]Hostapd (Host Access Point Daemon) user space software capable of turning normal wireless network interface cards into access points and authentication servers

According to the components available in the emulator, it was built the topology of Figure 4 . The radio access network is constituted by the OpenFlow enabled BS antennas, the RRHs, and the mobile users, the UEs. The backhaul consists on the forwarding switches, also OpenFlow enabled. In this context the node used as host simulates a server as an external network, in accordance with a LTE typical architecture, where the traffic can be directed. This is essentially used to test End-to-End services such as a connection between a UE and the Internet.

Network Components

The topology implemented in the emulator represents a simplified version of a LTE network meeting the C-RAN concept described in Chapter 2, and it is presented in Figure 5.

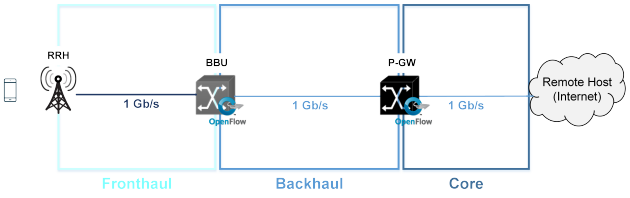

Figure 5: Mininet-Wifi architecture and components

The RRHs represent a simple base station antennas located at the cell sites. The BBUs, in this topology, are represented by OpenFlow virtualized switches. Each BBU serves 3 RRHs, and they are considered centralized since they can communicate with each other using the controller. The fronthaul link, between the RRH and the BBU is considered to be fiber, which seemed the most convenient choice due to fiber availability and applicability. The EPC network, regarding the user plane connections responsible for the packet transport, is reduced to routing-enabled elements. The control part of these network elements is responsibility of the controller.

The topology previously described and implemented in the emulator has the main components:

- **Controller**

  The POX [2] controller was used, a simple-to-use SDN controller that is bundled with *Mininet* and whose components are python programs that implement network functions and can be invoked when POX is started. It also creates network applications that performs switching based on Ethernet MAC addresses, and prevent loops in the network. The controller implements instructions in the switches to forward traffic, acting directly in their flow tables.

- **UEs** are the mobile users and they are connected to the RRHs through authentication and association. For each UE an IP and MAC addresses

are defined. In addiction to these addresses, the antenna gain and antenna height are also established.

- **RRHs** are the network elements responsible of maintain the UEs connected to the network and assure the communication between them and the controller. When the UEs enter in other access point range the user starts to be served by the new one, according to the association rules, which can give priority to the signal quality or RRH load. The association rule used is defined before the program execution.
- **Open vSwitch** are the switches used in the network and are an open-source implementation of a distributed virtual multilayer switch. These elements are the ones responsible for introducing virtualization in the network. In this particular network, the switches work as OpenFlow switches, and it is possible to see their flow tables at any time during the program execution.

3.2. LTE modules implementation

In the wireless network, between the mobile user and the serving base station antenna, it was necessary to implement some modules in order to the simulations be coherent with LTE. To do so, classes in python were added, or modified, in the scripts that constitute the software, to support the addition of the LTE devices and their features.

3.2.1 LTE Radio Frequency (RF) scenario

In order to test the SDN potential in LTE networks, a radio access network scenario from 3rd Generation Partnership Project (3GPP) [3] for LTE was used as reference. According to the reference scenario, the base stations with three sectors per site are placed in a hexagonal grid distanced of 3 × R, where R represents the cell radius. The BS antenna radiation pattern used for each sector in 3-sector cell sites depends on the horizontal angle. However, the original BS antennas from the emulator are omnidirectional, radiating in all directions and not taking into account the horizontal angle between the UE and the BS antenna. So in order to use the implemented code to simulate sector antennas, it was considered the direction of maximum gain of the radiation pattern, and the transmission antenna gain value it was defined according to the same reference [3].

For the RAN implementation, and further network tests, the parameters presented in Table 1 were used, for both urban and rural scenarios.

Beyond the radiation pattern, the transmission antennas in WiFi and LTE are different, so in order to use antennas as reliable as possible, a class was created in the emulator, in the script where the network devices were implemented, corresponding to the emulation of the LTE transmission antennas characteristics, the eNodeBs, with the features presented in Table 1.

Table 1: RAN parameters from [3]

Environment	Urban area	Rural area
Cell range	500 m	2000 m
Carrier frequency	2000 MHz	900 MHz
System bandwidth	10 MHz	10 MHz
BS antenna		
Antenna height	30 m	45 m
Antenna gain	15 dBi	15 dBi
Maximum BS power	46 dBm	46 dBm
User equipment		
Antenna height	1.8 m	
Antenna gain	0 dBi	
Maximum UE power	24 dBm	
UE noise figure	9 dB	

The primary adopted LTE component was the implementation of the macro cell propagation model. For urban areas, the model is valid for the Non Line of Sight (NLOS) case only and describing the worse propagation case. This model is based on the 3GPP reference [3] considering a carrier frequency of 2000 MHz and a base station antenna height of 15 metres above average rooftop level. The propagation model is given by the following formula:

$$L_{urban[dB]} = 128.1 + 37.6 \times \log_{10}(R_{[m]} \times 10^{-3}), \quad (1)$$

where R is the base station - user equipment distance.

In rural areas the Hata model from the same reference was used and, as for the urban case, is valid for the Non Line of Sight (NLOS) case only and describing the worse propagation case. Considering a carrier frequency of 900 MHz and a base station antenna height of 45 meters above ground the propagation model is given by:

$$L_{rural[dB]} = 95.5 + 34.1 \times \log_{10}(R_{[m]} \times 10^{-3}) \quad (2)$$

where R is the base station - user equipment distance.

The UE received power, which is useful to estimate the SNR, using the above path loss formulas for each environment, can be calculated by:

$$P_{r[dB]} = P_{t[dBm]} + G_{t[dBi]} + G_{r[dBi]} - L_{[dB]}, \quad (3)$$

where P_t represents the transmitter output power, G_t is the gain of the transmitting antenna, G_r is gain of the receiving antenna and L_p refers to the path loss.

3.2.2 Modulation and coding scheme

The Modulation and Coding Scheme (MCS) was used to determine the data rate of a connection, and even

though WiFi and LTE present spectral efficiency depending on the modulation coding scheme, they give different values of spectral efficiency for each MCS. In WiFi, spectral efficiency depends on the technology (e.g., 802.11a, 802.11b, 802.11n, etc.), and because of that, it was necessary to implement the LTE coding scheme index distribution.

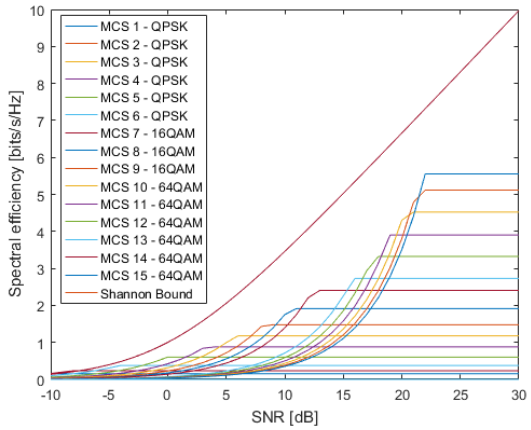

Figure 6: MCS Theoretical curves.

Using the LTE Channel Quality Indicator (CQI) Table from 3GPP [6], along with Equation (4) from [5], the spectral efficiency was plotted according to the SNR. The MCS curves were projected in Matlab® and are presented in the graph of Figure 6. The following equation was the equation used for plotting:

$$\frac{R_b}{B} = min(\frac{3\log_2 M}{2(M\text{-}1)(\text{erfc}^{-1}(\frac{P_{b,target}\log_2 M}{2}))^2}\frac{n}{k} \; G_{MCS}\,(P_{b,target})\,\text{snr}, \frac{k}{n}\log_2 M), \quad (4)$$

where M is the number of bits per modulation symbol (e.g., QPSK (M=4), 16-QAM (M = 16) and 64-QAM (M = 64)) , G_{MCS} is the coding gain , $\frac{k}{n}$ is the code rate and snr is the signal to noise ratio, in linear units. The Bit Error Rate (BER) target, $P_{b,\,target}$, is 10^{-3}, since, using SISO, the system does not guarantee a BER smaller than the 10^{-3} BER target for SNR less than -10 dB as described in [5].

The MCS curves give the maximum rate supported in each modulation,for each SNR interval. This interval can be taken from the graph of Figure 6 and was implemented in the emulator.

3.3. Network Tests and Assessment
Considering the emulator' potential and limitations some assumptions were assessed:

- The BBUs, and the RRHs, are used as a representation to address the C-RAN concept for 5G networks. However, they do not execute explicit baseband, and digital, processing functions, respectively;
- The distance between RRHs and BBUs is not taking into account, once are assumed fiber links with high capacity and all signal processing is done at the RRH level, so this possible limitation do not affect the network performance;
- The core network is used in terms of packet forwarding, and the S-GW and P-GW control functions are executed at the SDN controller level;
- The end-to-end TCP/UDP connection is assumed to be similar for WiFi and LTE, according to both technologies' protocol stack;
- The NFV component of this work is represented by the use of virtual switches.

In the simulations in Mininet-Wifi, several tests were performed in order to see, not only the SDN influence in mobile networks, but also to test the feasibility of this approach. The network performance is measured in two classic ways: the network throughput and the packet latency, or Round Trip Time (RTT).

3.3.1 Throughput

Iperf [11] was the tool used for throughput measurements, which runs as an application and generates traffic. It measures the throughput between two points of the network (e.g. a mobile user and a host acting as a server) through TCP packets exchange. This two points were selected in order to simulate an E2E LTE connection. In order to take some conclusions regarding the network performance, the throughput values were converted to spectral efficiency, dividing the simulated results by the bandwidth. Plotting the spectral efficiency values according to each SNR, is possible to obtain a comparison with the Shannon bound curve.

The Shannon bound represents the capacity of an Additive White Gaussian Noise (AWGN) channel and therefore, the maximum theoretical spectral efficiency that can be achieved in LTE. It can be expressed as:

$$C_{[\text{bits/s/Hz}]} = B_{[\text{MHz}]} \times \log_2(1 + \text{snr}), \quad (5)$$

where C is the Shannon capacity, B the system bandwidth and snr the signal-to-noise ratio in linear units.

3.3.2 Latency

In LTE there are two types of latency, the control plane latency and the user plane latency. The latency tests performed are only related to the user plane latency, usually defined by RTT which impacts the Quality of Experience (QoE).

The RTT measurements performed in the emulator are performed in two different ways:

1. In an E2E connection.

   The measurements to find the E2E latency of LTE networks for data applications are based

on the *ping* Round Trip Time (RTT). The RTT measures the time between sending and receiving Internet Control Message Protocol (ICMP) messages (*ping* messages), between the terminal and the destination. In this case, the test was executed between a mobile terminal and an IP host, which is configured to respond to ICMP Echo Requests.

2. In a wired connection.

   The *ping* test is is executed in the same way as the previous test, but this time between the IP host and the base station antenna.

3.3.3 Hypotheses Assessment

The metrics used to assess the validity of each test were the Root Mean Square Error (RMSE), the Pearson Correlation coefficient and the R-squared; however, the only values presented in this paper are the RMSE, since the other two metrics present values very close to 1. The RMSE measures the difference between the predicted and the true values. The Pearson coefficient assesses the linear correlation between the original and the estimated values. The R-squared is a measure of how close the data is to the fitted curve line.

4. Result Analysis

This chapter presents the results of the performed tests in order to evaluate the network performance. These results are then analysed and compared to field measurements.

4.1. Throughput

The first performed test aimed to understand the network behaviour considers the throughput. The UE was placed manually in a position, corresponding to a certain SNR value, and a throughput measurement was done during 60 seconds, from which, minimum, maximum and mean throughput values were obtained. The same process was applied in several terminal positions, equally spaced, in order to scan the throughput within the SNR interval [-5;30] dB.

The graph of Figure 7 was obtained from the average throughput measurements at each position, divided by the corresponding channel bandwidth (10 MHz), resulting in the spectral efficiency, for a urban environment.

In order to get a spectral efficiency curve (by fitting the experimental data), the following function, representing an attenuated and truncated form of the Shannon bound, was used:

$$\frac{R_b}{B}(\eta_{BW,r}, \eta_{SNR,r})_{[bits/s/Hz]} = \eta_{BW,r} \times \log_2(1+\eta_{SNR,r} \times snr), \quad (6)$$

where snr represents the signal-to-noise ratio in linear units and the coefficients $\eta_{BW,r}, \eta_{SNR,r}$ are related to the bandwidth and snr efficiencies respectively.

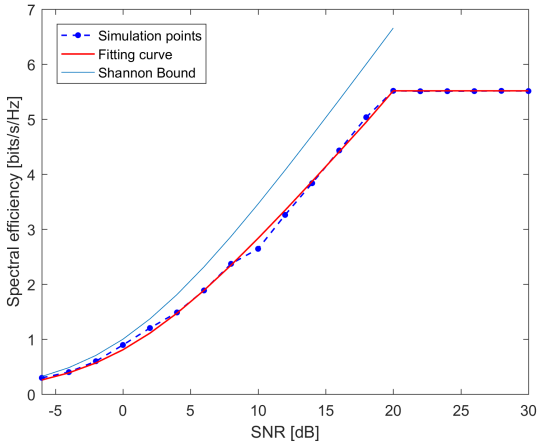

Figure 7: Spectral efficiency obtained in the emulator for an urban environment.

According to (6) and using Matlab® to approximate the data points to a fitting curve capable of being compared with the Shannon bound equation, the coefficients presented in 2 were obtained.

Table 2: Throughput fitting results for an Urban environment

SNR	$\eta_{BW,r}$	$\eta_{SNR,r}$	RMSE
[-4, 20] dB	0.83234	0.96005	0.0783

In Figure 7 the Shannon bound is represented in light blue; since the LTE bandwidth efficiency is reduced by several factors, presented in Table 3, this capacity limit is never reached.

Table 3: Bandwidth efficiency for 10 MHz LTE system downlink [14]

Impairment	Link $\eta_{BW,r}$	System $\eta_{BW,r}$
BW efficiency	0.9	0.9
Cyclic Prefix	0.93	0.93
Pilot overhead	-	0.94
Dedicated and common control channels	-	0.715
Total	**0.83**	**0.57**

In [14], the authors simulated an Additive White Gaussian Noise (AWGN) channel with 10 MHz bandwidth in a Typical Urban (TU) environment and an overall link bandwidth efficiency of 83 % was found, where the $\eta_{SNR,r}$ was obtained by curve fitting. Including the additional system level overhead, the LTE bandwidth efficiency of the shared data-channel becomes 57 %. The same reference also presents the values which provides the best fit to the link adaptation curve, corresponding to a bandwidth and SNR efficiencies of 0.75 and 0.8 respectively.

The two modified Shannon curves resulting from the coefficients obtained in [14] are represented in Figure 8 along with the curve obtained in the emulator and the Shannon capacity bound.

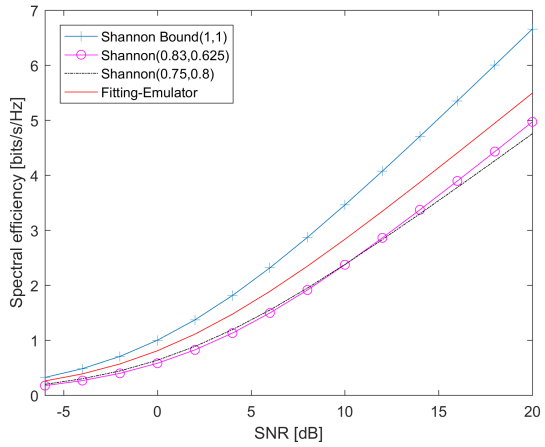

Figure 8: Throughput fitting curves comparison.

As one can see, the emulator constantly displays higher values of spectral efficiency, once the graph has no negative values. The maximum difference achieved for the 83% efficiency curve was 0.46 dB and 0.94 dB regarding the curve which takes the AWGN efficiency into account. For the bandwidth considered (10 MHz), that difference corresponds to a difference in throughput of 4.6 Mbit/s and 9.4 Mbit/s (8.2 % and 16.8 %, respectively).

The spectral efficiency values presented in the graph of Figure 9 were obtained from the average throughput measurements, as for the urban environment, but this time, for the rural scenario.

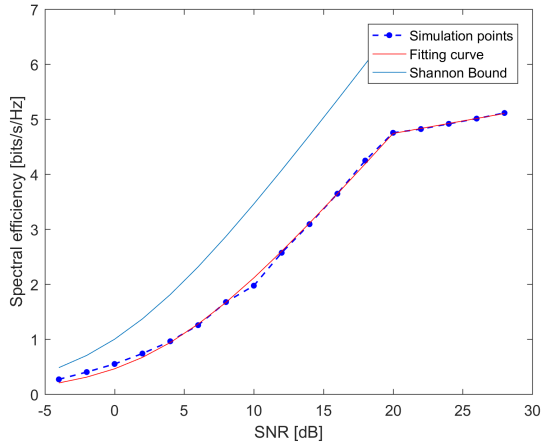

Figure 9: Spectral efficiency obtained in the emulator.

The parameters obtained from the curve fitting are presented in Table 4.

The throughput measurements in this environment does not stabilize for SNR values greater than 20 dB.

Table 4: Throughput fitting results

SNR	$\eta_{BW,r}$	$\eta_{SNR,r}$	RMSE
[-4, 20] dB	0.85722	0.4532	0.0682

Instead, for the highest modulation which imposes a maximum spectral efficiency of 5.6 bits/s/Hz, the throughput, and consequently the spectral efficiency, increases linearly, but never reaching the maximum rate. The spectral efficiency requirements for the urban and rural scenarios tested, according to [17] are presented in Table 5.

Table 5: Average spectral efficiency comparison

Environment	Emulator [bits/s/Hz]	ITU requirement [17] [bits/s/Hz]
Urban Macro	**3.4**	**2.2**
Rural Macro	**2.84**	**1.1**

Can be concluded that, using a SDN emulator and a LTE radio network, the spectral efficiency values are better than the ones imposed by international entities. For the urban scenario, the proposed solution presents an increase of 54 % regarding the ITU requirement, and for the rural environment an increase of 158 % was achieved.

4.2. Latency

The second test addressed the E2E latency based on the ping test, which measures the RTT, and, like in the throughput test, a fitting curve was calculated in order to analyse how latency varies with SNR. The tests were performed for three packet sizes (32, 1000 and 1500 bytes), to see how this parameter affects the network performance. The same procedure was done for two difference environments : Urban and Rural.

The latency was measured from the cell edge to the center in equal spaced time intervals, corresponding to the SNR values mapped in the figures 10(a) and 10(b), for the urban and rural environments respectively. In the graphs of the aforementioned figure, the outliers were removed. These outliers happened periodically, corresponding to the OpenFlow hard timeout, starting in the first exchanged packet. The hard timeout is presented in the Openflow flow entries and, as described in Chapter 2, it represents the maximum amount of time a flow stays in the switch. After that time, the flow expires and a new rule needs to be sent from the controller to add the entry again.

The fitting curves for latency, or RTT, presented in the graphs of Figure 10, dependent on SNR, resulted from equations of the form:

$$\mathrm{RTT}_{[\mathrm{ms}]} = \mathrm{b}_1 \, \mathrm{e}^{\mathrm{b}_2 \times \mathrm{SNR}}, \tag{7}$$

where SNR represents the signal-to-noise ration in dB in each position. The coefficients b_1 and b_2 depends on the packet size, since it is the only different condition from one curve to the other. These coefficients

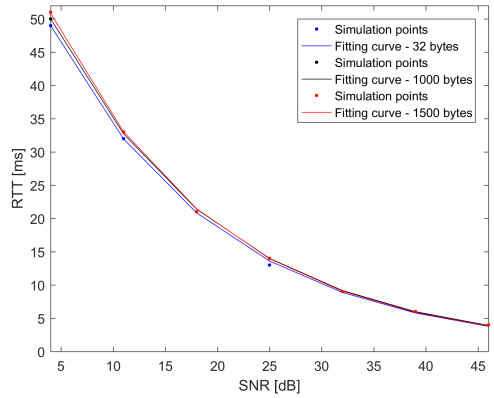

(a) Latency fitting curves - Urban Environment

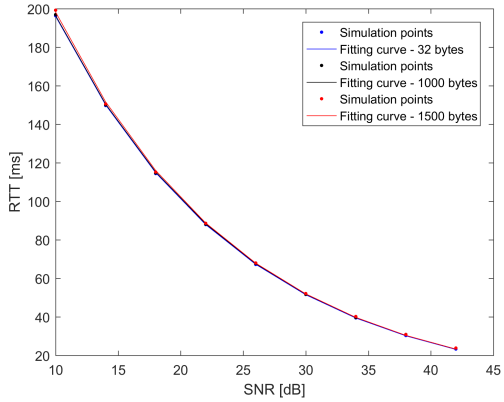

(b) Latency fitting curves - Rural Environment

Figure 10: Latency fitting curves according to packet size.

are presented in Table 6.

Table 6: Latency fitting coefficients

	Packet size (bytes)	b_1	b_2	RMSE
Urban	**32**	54.232	-0.05751	0.445
	1000	59.576	-0.059027	0.474
	1500	58.854	-0.055837	0.694
Rural	**32**	382.57	-0.066865	0.261
	1000	382.6	-0.066656	0.415
	1500	387.21	-0.066966	0.728

Analyzing the curves obtained for the BS range defined in the reference scenario and positioning the user according to an uniform distribution, it was achieved a minimum, average and maximum latencies as shown in Table 7. Assuming a E2E latency requirement of 20 ms, according to ITU [12], the following results can be extracted:

4.3. Use Case - Drive-Tests

In order to compare the latency results with real network measurements, a set of drive-tests were used, along with the network topology of Lisbon provided by a portuguese operator. Two types of drive-tests were used: one containing information regarding signal conditions, and other with RTT measurements. All drive-tests were used for the propagation model calibration and the second, containing the RTT information, served to compare the results measured with the ones obtained in the emulator.

Table 7: RTT comparison between emulator's tests

	Packet size (bytes)	Minimum (ms)	Average (ms)	Maximum (ms)
Urban	32	4.014	21.434	62.538
	1000	4.165	21.962	63.746
	1500	4.069	22.128	65.053
Rural	32	18.878	121.679	382.570
	1000	19.058	122.006	382.600
	1500	19.020	123	387.21

The Standard Propagation Model (SPM) is a model used for network planning when calibration is required. It was developed based on the empirical formulas of Hata propagation and it is appropriate for mobile channel characterization. Ignoring the effects of diffraction, clutter and terrain, the resulting path loss equation was used [16]:

$$L_{p[dB]} = k_0 + k_1 \log_{10}(f_{[MHz]}) + k_2 \log_{10}(h_{tx[m]}) + [k_3 + k_4 \log_{10}(h_{tx[m]})] \log_{10}(d_{[km]}), \quad (8)$$

where h_{tx} represents the base station height, d is the distance between the *drive-test* and the base station which is serving it, and f is the downlink channel frequency with a corresponding LTE E-UTRAN band. The constants k_0, k_1, k_2 and k_3, represent the parameters obtained by applying a fitting curve to the *drive-tests* data.

The *drive-tests* with the signal level were analyzed in two different areas of Lisbon (*Sapadores* and *Cidade Universitária*), according to the RTT *drive-tests* available. Each area gave rise to the k_i coefficients presented in Table 8.

Table 8: SPM coefficients and RMSE

Area	k_0	k_1	k_2	k_3	k_4	RMSE [dB]
1	56.16	17.24	41.24	14.39	10.57	9.15
2	1.88	49.75	1.33	12	8.48	6.04

Making an overall analysis of both scenarios, it can be extrapolated a general curve which includes all the RTT *drive-tests* available. The final curve is the result of the average latency of both scenarios at each point, and it is represented in Figure 11.

Despite the large number of *drive-tests* available, many were duplicated. Then, after the removal of the duplicated data, most had only RTT values, that is,

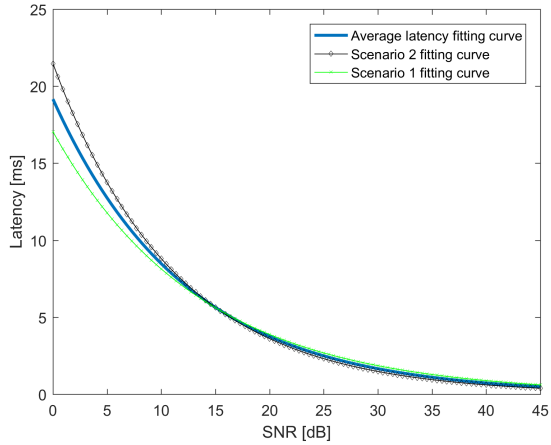

Figure 11: Latency curve obtained from scenarios 1 and 2.

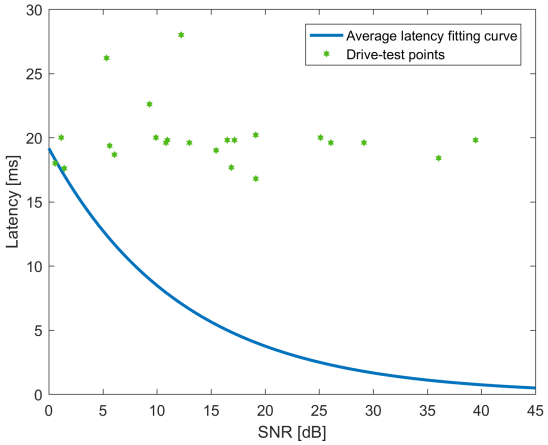

Figure 12: Latency curve obtained and RTT points from drive-tests.

they had no information regarding the signal power or the signal-to-noise ratio. So in order to use those values, the following strategy was adopted:

1. Latitude and Longitude extraction from both the *drive-test* and the cell site which has the same PCI, and calculate the distance between them;
2. Apply the SPM to obtain the path loss, followed by received power calculation;
3. Obtain the SNR with the received power, the transmission antenna parameters and the average of all *drive-tests*' noise;
4. Associate each RTT measurement to the corresponding SNR, and plot the *drive-tests*.

After applying these steps and having the SNR values for each *drive-test* it is possible to compare de RTT from the *drive-tests* with the curve obtained in the emulator. This comparison can be observed in the graph of Figure 12.

The different behaviour of the two curves is notorious. The *drive-tests* have constant latency values for any SNR, varying between 18 and 30 ms, and presenting an average of 20.24 ms. On the other hand, in the emulator it can be seen an exponential dependence between the latency and the SNR. This variation of latency, in the emulator, happens in the wireless part of the network, and it is directly related to how it is implemented. But even so, presents very low values.

An analysis was also made, in the emulator, for the wired part of the network, in order to see how the SDN impacts the packet flow and the latency times. Using the latency average value obtained in the emulator, corresponding to the RTT ($2 \times T_{S1\text{-}U}$), and ITU air latency, a comparison can be made with the *drive-tests* for each SNR value. Plotting the RTT values from the *drive-tests* along with the emulator RTT, which do not depend on the SNR, the results in Figure 13 were obtained.

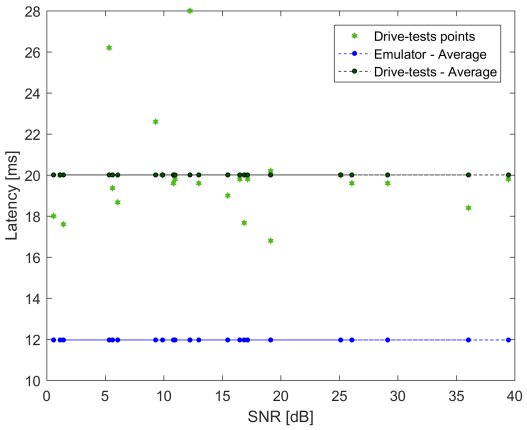

Figure 13: RTT comparison between *drive-tests* and Emulator/3GPP.

As one can see, the average latency obtained in the emulator is much lower than the values of the *drive-tests*; more specifically, 40.18 % lower. On the other hand, it can be verified that *drive-tests* latency is, mostly, lower than the value obtained by ITU.

5. Conclusions

The main goal was to evaluate the performance of a 4G network with SDN capabilities, and to do that, the Mininet-WiFi, an SDN emulator, was used to merge the mentioned technologies, towards a LTE RAN SDN based solution, which represents one of the strongest architectures concerning the 5G world.

The proposed approach crossed one major issue, which was the fact that the wireless part of the emulator, was implemented for WiFi networks. In order to adapt the emulator to this project needs, LTE modules were developed in the radio access network.

Starting with the throughput analysis, it was obtained a spectral efficiency curve, for each environment, which presented very good results of RMSE with a value of 0.0783 dB for the urban environment

and 0.0682 dB for rural. Analyzing the throughput regarding the network performance, the proposed solution for the urban environment, presented a 54 % spectral efficiency increase regarding the ITU requirement. For rural areas, it was obtained a 158 % spectral efficiency increase, also using ITU as reference.

Concerning the latency tests, an exponential dependence with SNR was obtained, for three packet sizes and the two environments used for the throughput tests. These tests also presented good RMSE, between the simulated points and the fitting curve obtained. The average latency obtained for the three packet sizes in urban environments stood at around 21-22 ms, and for the rural environment the latency rises to 120 ms. As an use case, *drive-tests* were used to compare the latency with real network measurements; they were initially applied to the calibration process of a propagation model, the SPM, which reflects the experimental environment (urban). The SPM was then implemented into the emulator. The latency measurements were then extracted from the emulator and compared with the drive-tests. The drive-tests latency is mostly constant, around 20 ms, with some punctual fluctuations within 18 ms and 30 ms, but SNR independent, while in the emulator, the latency results were considerably smaller but depended on the SNR.

References

[1] mac80211_hwsim. `https://wireless.wiki.kernel.org/en/users/drivers/mac80211_hwsim`, 01 2015. [Online; Accessed in 14-February-2018].

[2] Pox, 2015. `https://noxrepo.github.io/pox-doc/html/`[Online; accessed 30-April-2018].

[3] E. 3rd Generation Partnership Project (3GPP). Evolved universal terrestrial radio access (e-utra); radio frequency (rf) system scenarios (3gpp tr 36.942 version 10.2.0 release 10). *ETSI TR 136 942 V10.2.0 (2011-05)*, 2011. [Online; accessed 05-June-2017].

[4] H. L. Y. Y. S. L. K. G. B. M. S. D. L. Checko, Aleksandra; Christiansen. Cloud ran for mobile networksa technology overview. *IEEE Communications Surveys & Tutorials (Volume: 17, Issue: 1)*, 2015. [Online; accessed 29-April-2018].

[5] P. M. de Almeida Carvalho Vieira. *Spatial Multiplexing MIMO Capacity Enhancement for 4G Macro-cell Networks*. PhD thesis, Instituto Superior Tcnico, 2008.

[6] ETSI, 650 Route des Lucioles F-06921 Sophia Antipolis Cedex - FRANCE. *"LTE; Evolved Universal Terrestrial Radio Access (E-UTRA); Physical layer procedures (3GPP TS 36.213 version 8.8.0 Release 8)"*, 2009.

[7] O. N. Foundation. Openflow switch specification. *ONF TS-006*, 2012. [Online; accessed 18-May-2017].

[8] O. N. Foundation. Software-defined networking: The new norm for networks, 04 2012. ONF White Paper.

[9] M. Jammal, T. Singh, A. Shami, RasoolAsal, and Y. Li. Software-defined networking: State of the art and research challenges. *Submitted for review and possible publication in Elseviers Journal of Computer Networks*, 2016. [Online; accessed 18-May-2017].

[10] M. Jarschel, T. Zinner, T. Hofeld, P. Tran-Gia, and W. Kellerer. Interfaces, attributes, and use cases: A compass for sdn. *IEEE Communications Magazine*, 2014. [Online; accessed 19-May-2017].

[11] E. . L. B. N. Laboratory. Iperf, 2003. `https://iperf.fr/`[Online; accessed 17-January-2018].

[12] I.-R. M.2134. Requirements related to technical performance for imt-advanced radio interface(s), 11 2008.

[13] I. R. T. B. S. Mads Lauridsen, Lucas Chavarra Gimnez and P. Mogensen. From lte to 5g for connected mobility. *IEEE Communications Magazine (Vol: 55, Issue: 3)*, 03 2017.

[14] I. Z. K. F. F. A. P. K. I. P. T. K. K. H. Preben Mogensen, Wei Na and M. Kuusela. Lte capacity compared to the shannon bound. *Vehicular Technology Conference, Ed: 65*, 2017. [Online; accessed 05-March-2018].

[15] C. R. E. R. Ramon dos Reis Fontes. Mininet-wifi software, 2018. `https://github.com/intrig-unicamp/mininet-wifi`[Online; accessed 28-April-2018].

[16] N. F. C. T. C. E. A. Segun I. Popoola, Aderemi A. Atayero and V. O. Matthews. Calibrating the standard path loss model for urban environments using field measurements and geospatial data. *The 2017 International Conference of Wireless Networks*, 2017. [Online; accessed 26-April-2018].

[17] M. B. Stefania Sesia, Issam Toufik. *LTE The UMTS Long Term Evolution: From Theory to Practice*. John Wiley & Sons, Ltd, 2 edition, 2011. ISBN: 978-0-470-66025-6.

[18] M. Team. Mininet software, 2017. `http://mininet.org/`[Online; accessed 09-May-2017].

[19] I. technologies. Towards 5g ran virtualization enabled by intel and astri. White Paper, 2017. [Online; Accessed in 29-April-2018].